Supporting Figures for "Polymorph-specific kinetics and thermodynamics of β-amyloid fibril growth", by W. Qiang, K. Kelley, and R. Tycko

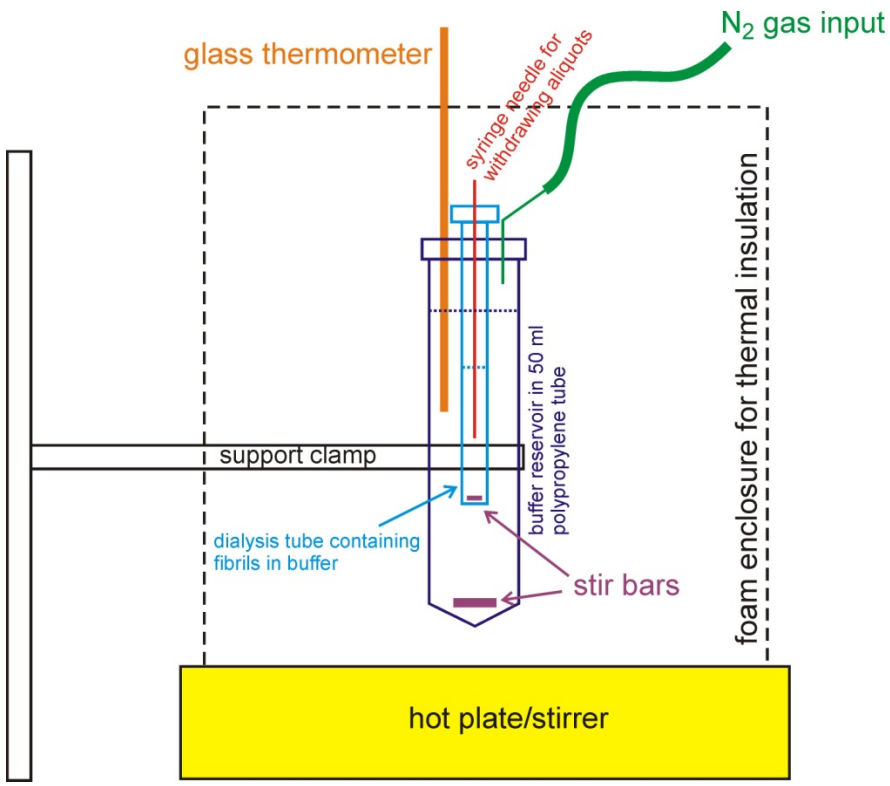

Figure S1: Schematic diagram of dialysis apparatus used for measurements of fibril shrinkage and quasi-equilibrium solubility. In the latter measurements, a larger quantity of fibrils was placed in the dialysis tube, and aliquots were taken from the buffer reservoir (rather than from the dialysis tube) for UV/HPLC analysis.

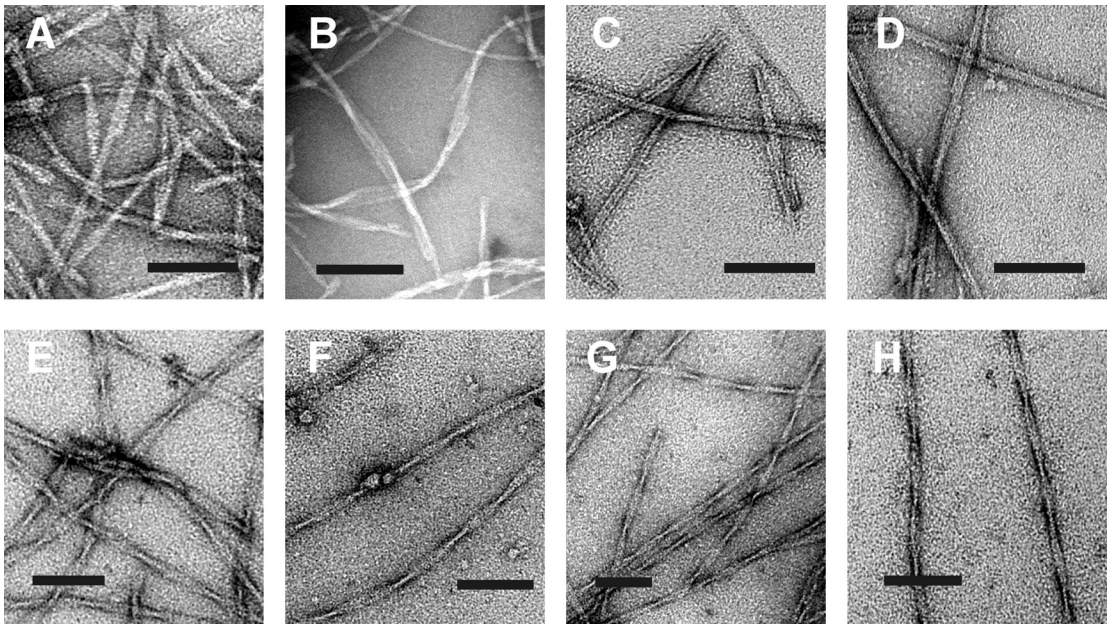

Figure S2: Representative TEM images of α (A-D) and α (E-H) $A\beta_{1\text{-}40}$ fibrils used as the source of seeds for fibril elongation measurements. Scale bars are 100 nm.

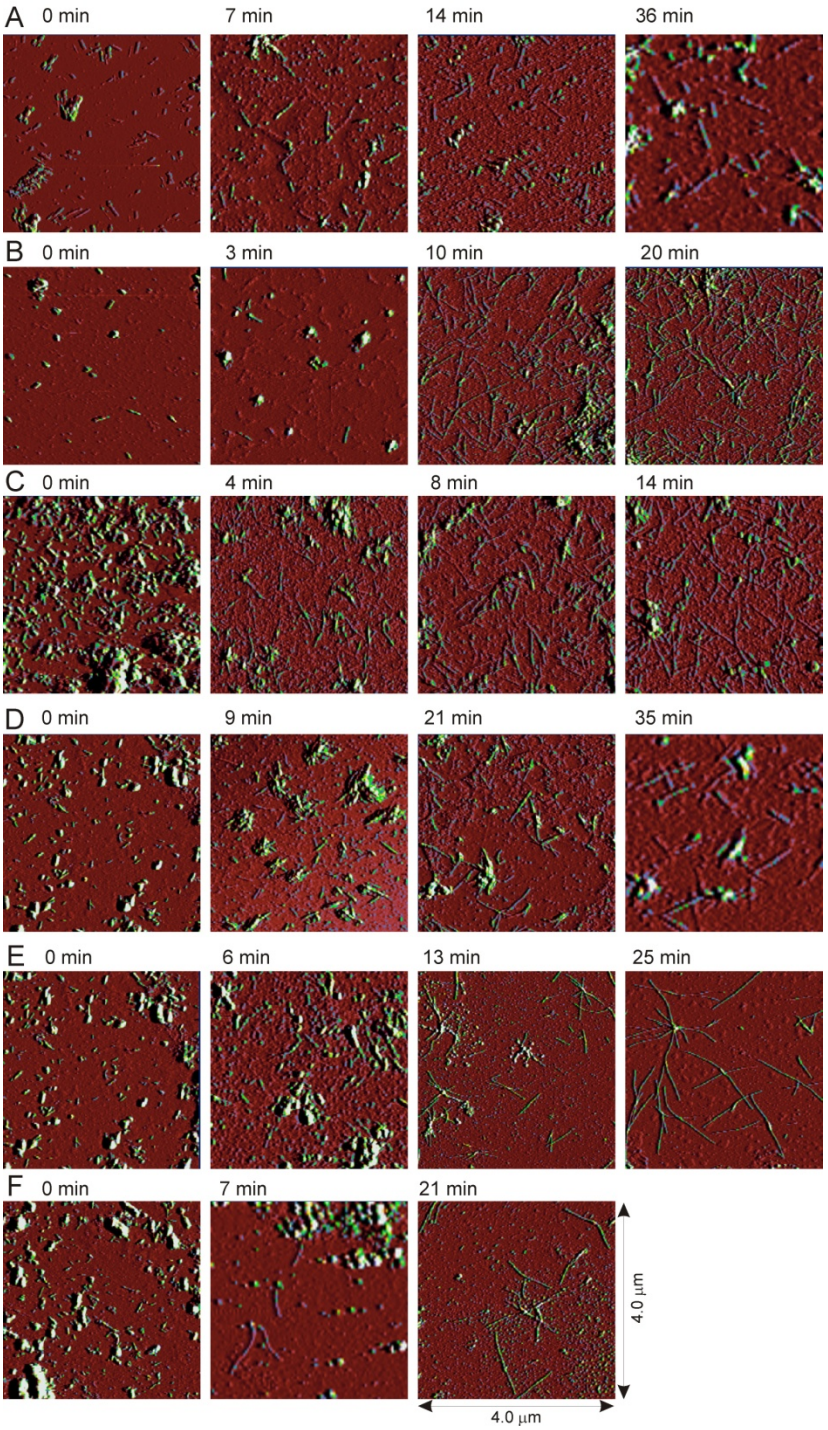

Figure S3: Representative AFM images (4.0 µm X 4.0 µm) from elongation measurements at 24° C. (A,B,C) $\mathcal{Q}$ fibril seeds with soluble $A\beta_{1\text{-}40}$ concentrations of 25 µM, 50 µM, and 75 µM, respectively. (D,E,F) $\mathcal{A}$ fibril seeds with soluble $A\beta_{1\text{-}40}$ concentrations of 25 µM, 50 µM, and 75 µM, respectively.

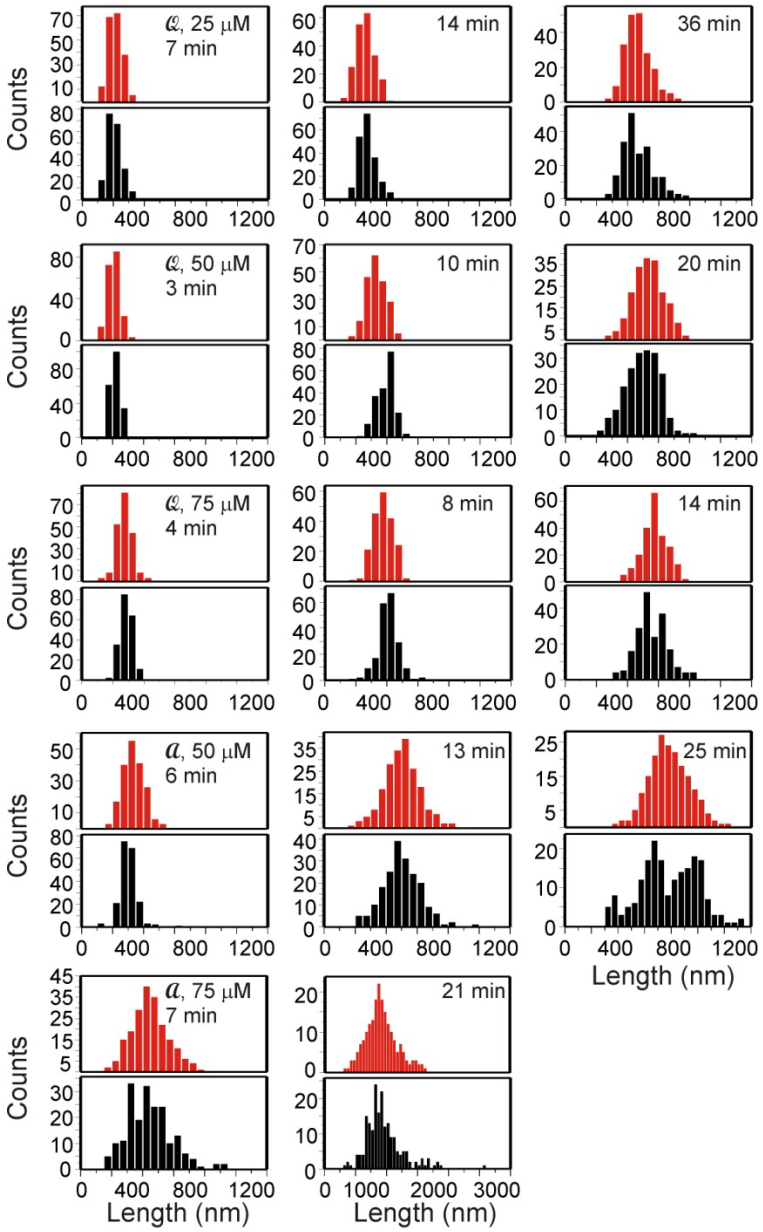

Figure S4: Experimental (black) and best-fit simulated (red) histograms of fibril length distributions at 24° C. $\mathcal{Q}$ and $\mathcal{A}$ represent "quiescent" and "agitated" fibril seeds.

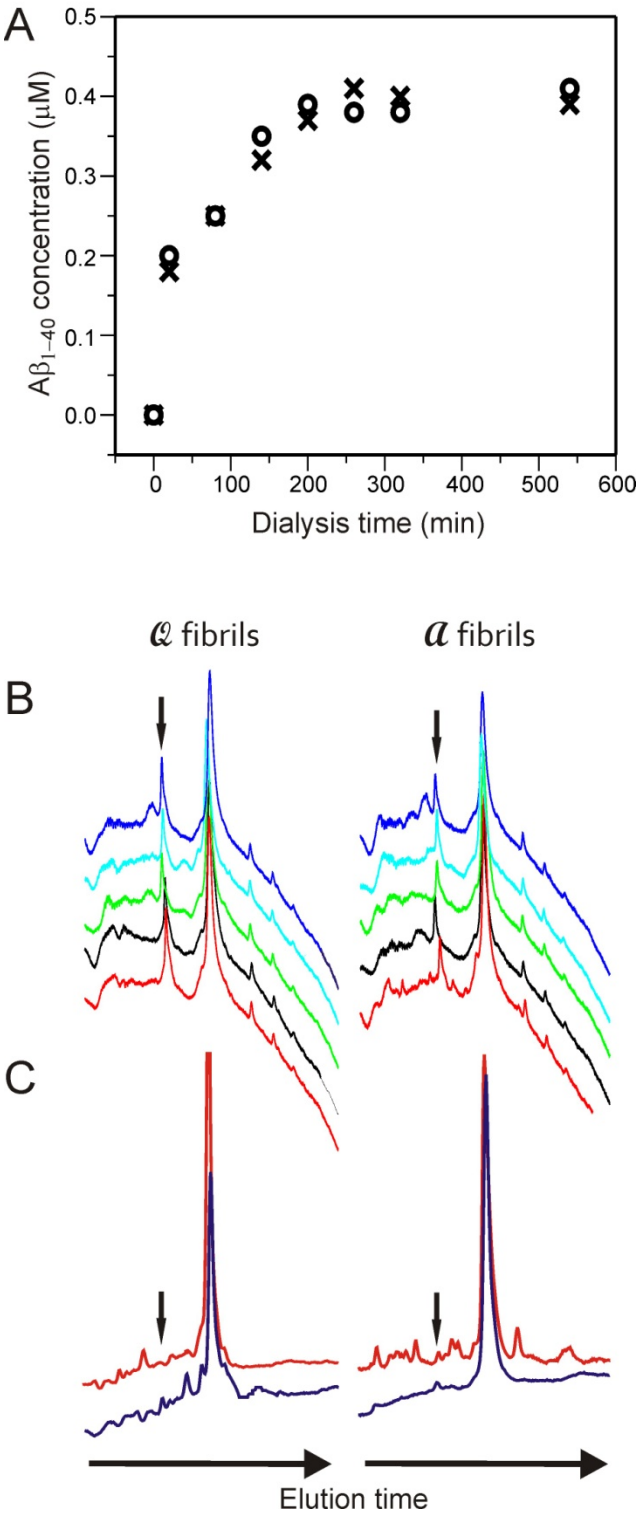

Figure S5: (A) Control experiment to show that monomeric $A\beta_{1-40}$ diffuses through the dialysis membrane used in quasi-equilibrium solubility measurements within 3 hr. Concentration in the buffer reservoir outside the dialysis tube is plotted as a function of dialysis time. Initial concentration of monomeric $A\beta_{1-40}$ inside the dialysis tube was 20 μM. Inner and outer buffer volumes were 1 ml and 45 ml, respectively. Circles and crosses represent two independent measurements. (B) HPLC traces from five independent measurements of quasi-equilibrium $A\beta_{1-40}$ monomer concentrations in the presence of *ℓ* and *a* fibrils at 24° C. Arrows indicate the position of the $A\beta_{1-40}$ elution peaks, which were identified by MALDI-TOF mass spectrometry. (C) HPLC traces from two independent attempts to measure quasi-equilibrium monomer concentrations at 37° C. The concentrations were below the reliable detection limit.

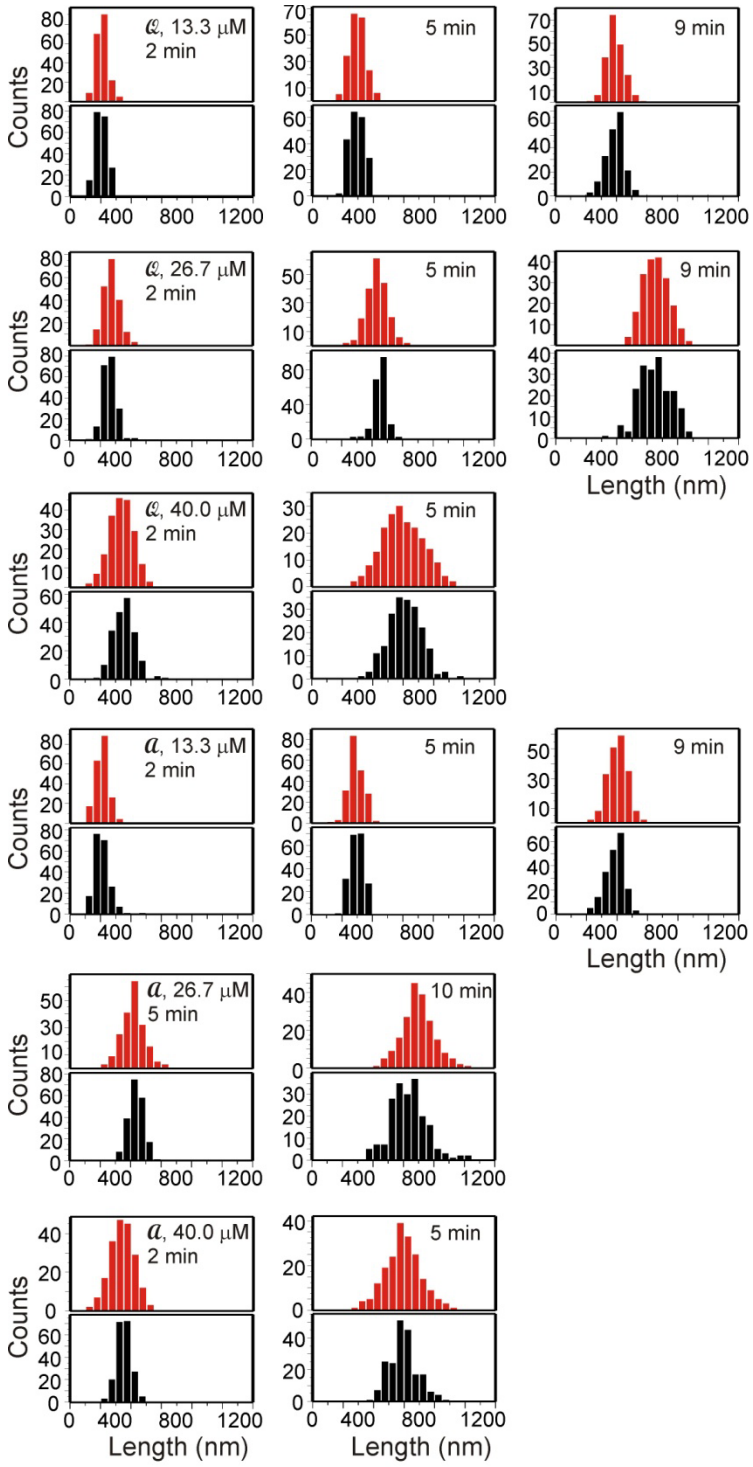

Figure S6: Experimental (black) and best-fit simulated (red) histograms of fibril length distributions at 37° C. $\mathcal{Q}$ and $\mathcal{A}$ represent "quiescent" and "agitated" fibril seeds.

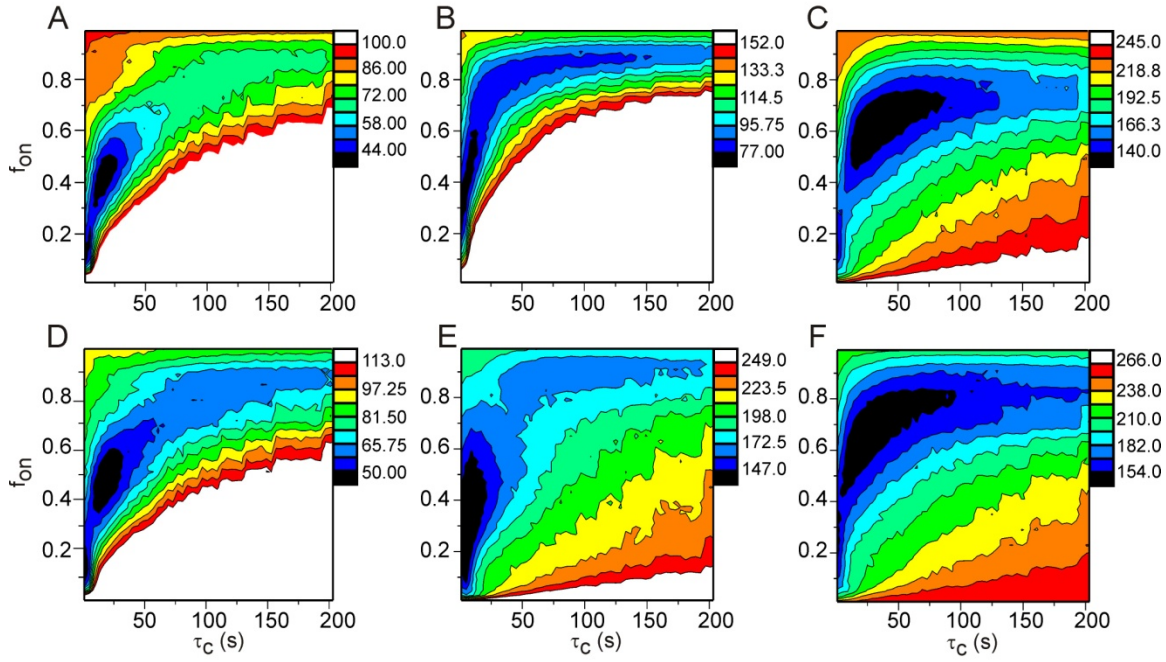

Figure S7: Same as Figure 6 of the main text, but for fibril elongation measurements at 37° C. (A,B,C) $\mathcal{Q}$ fibrils with 13 μM, 27 μM, and 40 μM soluble $A\beta_{1\text{-}40}$ concentrations, respectively. (D,E,F) $\mathcal{A}$ fibrils with 13 μM, 27 μM, and 40 μM soluble $A\beta_{1\text{-}40}$ concentrations, respectively.

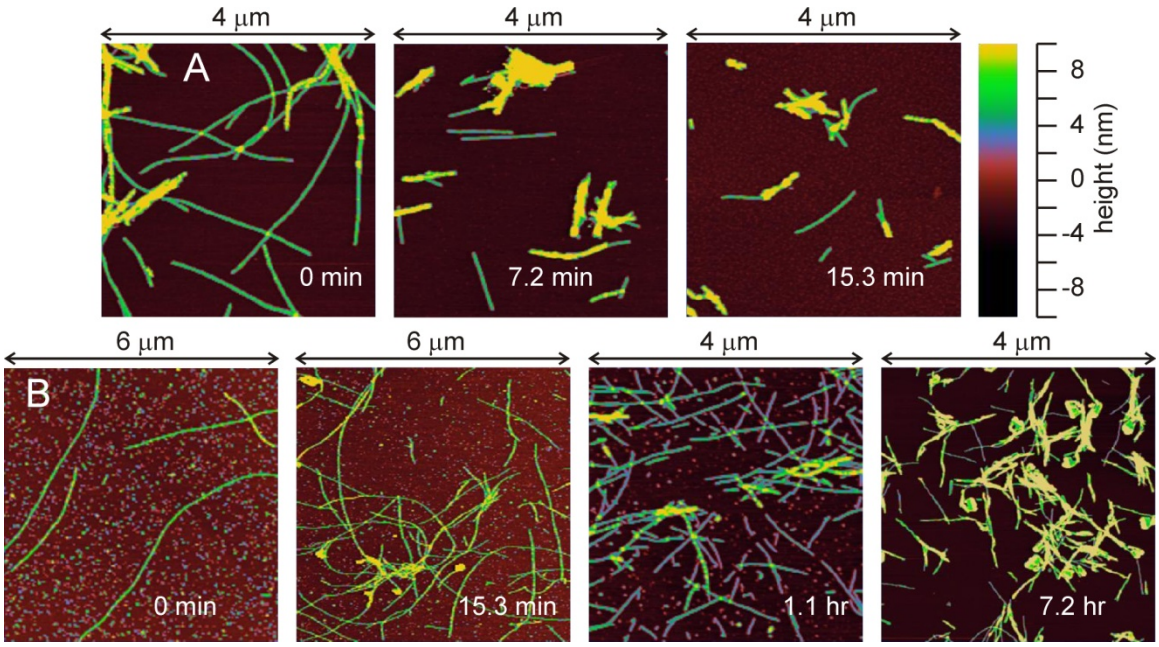

Figure S8: Polymorph-specific susceptibility to fragmentation by shear forces. Either $\mathcal{a}$ (A) or $\mathcal{Q}$ (B) $A\beta_{1\text{-}40}$ fibrils were suspended in incubation buffer in a 2 ml glass vial. A stir bar (6.6 mm length) was placed in the bottom of the vial and rotated at maximum speed with a stirrer plate (Corning model PC-410, setting 10) at 24° C. Aliquots were taken at indicated times, adsorbed to mica, and imaged in air by AFM. Height images are shown. Fragmentation of $\mathcal{a}$ fibrils was significantly more rapid than fragmentation of $\mathcal{Q}$ fibrils.